Chinese Chemical Letters 33 (2022) 3456–3460

Contents lists available at ScienceDirect

Chinese Chemical Letters

journal homepage: www.elsevier.com/locate/cclet

Visualized uranium rapid monitoring system based on self-enhanced electrochemiluminescence-imaging of amidoxime functionalized polymer nanoparticles

Ziyu Wang[a], Hang Gao[b], Peng Liu[a], Xinqi Wu[a], Qian Li[a], Jing-Juan Xu[b,*], Daoben Hua[a,c,*]

[a] State Key Laboratory of Radiation Medicine and Protection, School for Radiological and Interdisciplinary Sciences (RAD-X), Soochow University, Suzhou 215123 China
[b] State Key Laboratory of Analytical Chemistry for Life Science, School of Chemistry and Chemical Engineering, Nanjing University, Nanjing 210023, China
[c] Collaborative Innovation Center of Radiological Medicine of Jiangsu Higher Education Institutions, Soochow University, Suzhou 215123, China

ARTICLE INFO

Article history:
Received 5 September 2021
Revised 27 October 2021
Accepted 1 November 2021
Available online 11 November 2021

Keywords:
Visualized monitoring
Electrochemiluminescence
Amidoxime
Uranium
Public security

ABSTRACT

The development of uranyl ion detection technology has exhibited its significance in public security and environmental fields for the radioactivity and chemical toxicity of uranyl ion. The WHO standard of uranyl ion makes it necessary to develop highly sensitive uranyl rapid warning system in drinking water monitoring. Herein, a visualized rapid warning system for trace uranyl ion is carried out based on electrochemiluminescence (ECL) imaging technology to give an ultra-low limit of detection (LOD) and high selectivity. Amidoxime, a bi-functional group with both uranyl ion capturing and co-reactive functions, is modified on a conjugated polymer backbone with strong ECL signal to be prepared into three-in-one polymer nanoparticles (PNPs) with self-enhanced ECL property. The captured uranyl ion can enhance the ECL signal of PNPs *via* resonance energy transfer process to give the LOD as 0.5 ng/L, which is much lower than the known luminescent uranyl sensors. Furthermore, ECL imaging technology is introduced into realizing visualized uranyl rapid warning, and can be successfully applied on natural water samples. This study provides a novel strategy for uranyl rapid warning, and shows its potential meaning in public security and environmental fields.

Nowadays, nuclear power has exhibited its significance in providing large amounts of energy without producing greenhouse gases [1], taking up about 10% of the global power according to the statistics of the World Nuclear Association. As a kind of main nuclear fuel, uranium has been widely applied in nuclear power plants, which is also regarded as a hazardous element with long half-life (450 million years) as well as high radioactivity and chemical toxicity [2]. Due to some human activities such as mining and war, billions of tons depleted uranium ores, residues and weapons have been abandoned, which has become a large threat to environment and human's health [3]. As the most stable form of uranium in environment, uranyl ion (UO_2^{2+}) is severely limited in drinking water sources by the World Health Organization (WHO, less than 30 μg/L) [2]. Therefore, it is necessary to develop an accurate and rapid sensing system for the uranium warning of drinking water sources.

The most widely applied detection method of UO_2^{2+} is inductively coupled plasma-mass spectrometry (ICP-MS), which is the only approved method in WHO drinking water standard. Although ICP-MS can obtain quite low limit of detection (LOD, 10 ng/L), the instrument of ICP-MS is too large to conduct the rapid measurement in the wild. The complex operation is another reason for limiting ICP-MS in the application of UO_2^{2+} warning of drinking water sources. On the other hand, various kinds of UO_2^{2+} sensors have also been reported in the past several years, including fluorescent probes [4], electrochemical detection [5], colorimetric determination [6], DNAzymes [7] and so on. However, these techniques often suffer from low-sensitivity and complex operation, and cannot well meet the requirements of rapid uranium warning.

Electrochemiluminescence (ECL) involves an electron transfer process on the surface of electrodes to give excited states for luminescent signals, which can exhibit high sensitivity due to the ability to avoid scattered light and auto-luminescence backgrounds [8–11]. Except for this advantage, the simple operation and minimized instruments can also make ECL an outstanding choice in uranium warning system. Till now, ECL sensors have been employed in trace

* Corresponding authors.
E-mail addresses: xujj@nju.edu.cn (J.-J. Xu), dbhua_lab@suda.edu.cn (D. Hua).

https://doi.org/10.1016/j.cclet.2021.11.019
1001-8417/

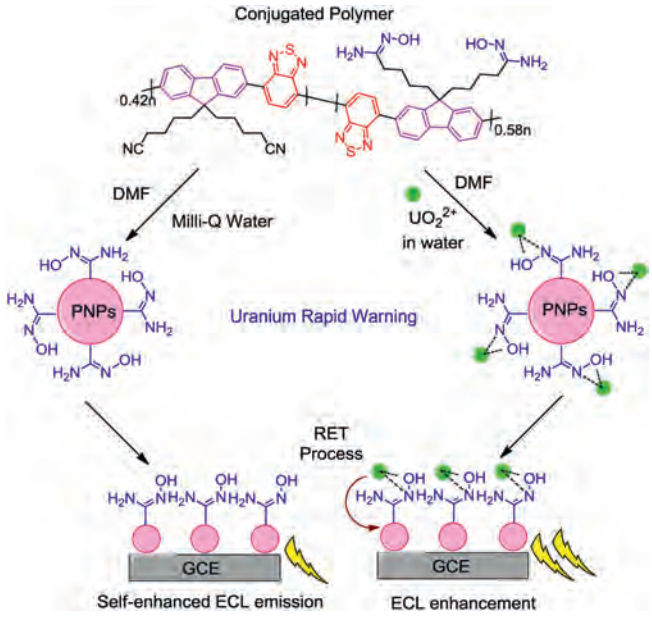

Scheme 1. Mechanism of self-enhanced ECL imaging sensor for uranium rapid warning.

detection of various heavy metals, such as Pb^{2+} [12], Hg^{2+} [13], Cu^{2+} [14]. Among them, we discovered the anodic ECL behavior of UO_2^{2+} and firstly developed a ssDNA based ECL sensor for UO_2^{2+} detection with quite high selectivity and sensitivity (LOD: 2.5 ng/L, lower than ICP-MS detection) [15]. This is the first research for applying ECL technology in trace radioactive substances detection, which carried out a brand new and efficient strategy for accurate UO_2^{2+} monitoring in environment [15]. However, due to the complex modification, pretreatment and data analysis, this strategy still could not meet the requirements of rapidity, intuition and simplification requirement in the UO_2^{2+} warning of natural water sources.

ECL imaging technique, based on traditional ECL technology, has been successfully applied in different fields such as biomolecular detection [16], cell imaging [17,18]. Compared to the traditional ECL technology, the color charged coupled devices (CCDs) can directly capture ECL images, which is beneficial for the rapid recognition by naked eyes [19]. Due to this advantage, ECL imaging sensors could be regarded as an excellent choice for UO_2^{2+} rapid warning. On the other hand, sensors with self-enhanced ECL behavior have also been applied in various fields due to their eco-friendly advantage of avoiding co-reactant reagents [18,20,21]. Therefore, designing ECL-imaging UO_2^{2+} sensors with self-enhanced ECL behavior has exhibited its significance in development of rapid uranium warning system, which has been rarely studied by previous works.

Herein, we reported a novel rapid uranium visualized warning system for drinking water source based on self-enhanced ECL imaging sensor modified by bi-functional amidoxime group (Scheme 1). Amidoxime has been regarded as one of the most successful UO_2^{2+} capturing groups with high selectivity in designing UO_2^{2+} adsorbents and has been widely applied in the extraction of uranium from seawater and the treatment of uranium-bearing wastewater [22–24]. The experimental data confirmed that the combination points of UO_2^{2+} in amidoxime group are the oxygen and nitrogen atoms of the oximido part (Scheme 1) [25]. In this work, we discovered that the amidoxime group can be applied as a co-reactive group in ECL sensing, making it a bi-functional group in newly designed UO_2^{2+} sensor. On the other hand, a commercial available conjugated polymer poly[(9,9-dioctylfuor-enyl-2,7-diyl)-*alt*-*co*-(1,4-benzo-{2,1′,3}-thiadiazole)] (PFBT) was chosen as the ECL emission backbone as well as fitting for ECL imaging detection due to its strong ECL signal [26]. After prepared into polymer nanoparticles (PNPs), the obtained three-in-one PNPs (combining luminogen, co-reactive group and UO_2^{2+} capturing parts) exhibited obvious self-enhanced ECL behavior as well as high sensitivity and selectivity to UO_2^{2+} *via* a resonance energy transfer (RET) process from UO_2^{2+} to PNPs. This PNPs can give an ultra-low limit of detection (LOD) value as 0.5 ng/L, which is at least three orders of magnitude lower than the known UO_2^{2+} fluorescent probes while five times lower than ssDNA based ECL sensor reported in our previous study (Table S1 in Supporting information) [15]. Furthermore, it was successfully applied in ECL imaging based UO_2^{2+} visualized rapid recognition for water samples from Xuan-Wu Lake (Nanjing, China), Gu-Cheng Lake (Nanjing, China) and Yangtze River (Yangzhou, China), respectively. This result indicates the practical application of this ECL imaging system in environmental and public security fields. What is more, this work is the first example of ECL imaging technology based UO_2^{2+} warning system, providing an accurate, simple and rapid strategy for radioactive elements warning in environment.

The detailed synthesis procedures of model polymer and conjugated polymer have been supplied in Supporting information while the synthetic routine was carried out in Scheme 2. The compounds **1, 2** and monomer **M-2** are commercially available while the monomer **M-3** was synthesized *via* previous literature [27]. The ^1H and ^{13}C NMR spectra of **M-1, P-1**, model polymer and conjugated polymer have been listed in Figs. S2-S6 (Supporting information) and GPC data were outlined in Supporting information too. As shown, the conjugated polymer and model polymer gave the yields as 72% and 76% while the M_w = 40,880 and 43,230, M_n = 21,040 and 27,320 as well as PDI = 1.94 and 1.58, respectively. In Fig. S2, the 4H triplet peak centered at 2.13 ppm can be assigned to -CH_2CN group of **M-1**, indicating that the 4H peak around 2.38 ppm in Fig. S4 can be assigned to the -CH_2CN group of **P-1**. While this peak changed into 1.7H in the ^1H NMR spectrum of conjugated polymer (Fig. S5), indicating that the modification ratio of amidoxime group can be calculated as (4H-1.7H)/4H = 0.58. On the other hand, a new peak appeared at 5.24 ppm containing 2.3H (Fig. S5), which can be regarded as the -CH_2- group combining with amidoxime group. This phenomenon can be regarded as another evidence for the successful modification of amidoxime group. This three-in-one conjugated polymer contains three parts with different functions: i) the conjugated backbone as the ECL emission part; ii) the -NH_2 in amidoxime group as the co-reactive group; iii) the -C=N–OH in amidoxime group as the UO_2^{2+} capturing group.

The conjugated polymer was then prepared into PNPs to give a concentration of 100 mg/L in Milli-Q water. It could be observed that the PNPs gave average diameter as about 50 nm (Fig. 1A). The conjugated polymer PNPs gave a strong anodic ECL signal without additional co-reactant with the onset potential at +1.13 V as well as the emission peak at +1.28 V, respectively (Fig. 1B). The ECL efficiency value of PNPs was calculated as 3.3% versus $[Ru(bpy)_3]^{2+}$ (10 μmol/L)/TPrA (25 mmol/L) system in a phosphate buffer saline (PBS) solution (0.1 mol/L, pH 7.4). To demonstrate the ECL emission process, the ECL emission backbone was synthesized without amidoxime group as model polymer (Scheme 2). The model polymer PNPs was prepared *via* the same process as conjugated polymer PNPs. In Fig. S7 (Supporting information), the cyclic voltammetry (CV) data of model polymer PNPs gave an obvious oxidation peak at +1.30 V, which is quite similar to the ECL emission peak of conjugated polymer PNPs (+1.28 V). This phenomenon indicated that the ECL emission can be attributed to the oxidation of the conjugated backbone in PNPs. In the CV data of conjugated polymer PNPs (Fig. 1C), two oxidation peaks can be observed at +1.18 V and +1.46 V with the onset potential at +1.05 V, respectively. The onset potential of ECL is higher

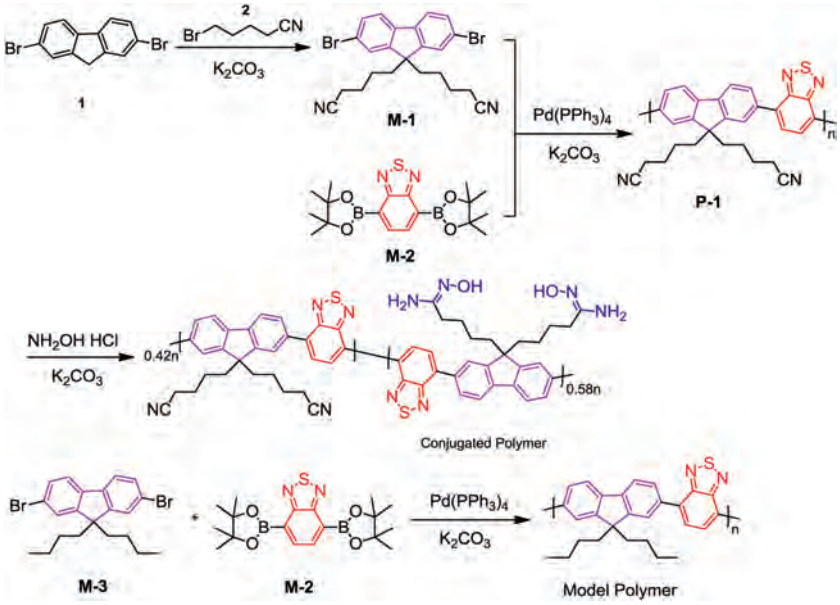

Scheme 2. The synthetic routine of model polymer and conjugated polymer.

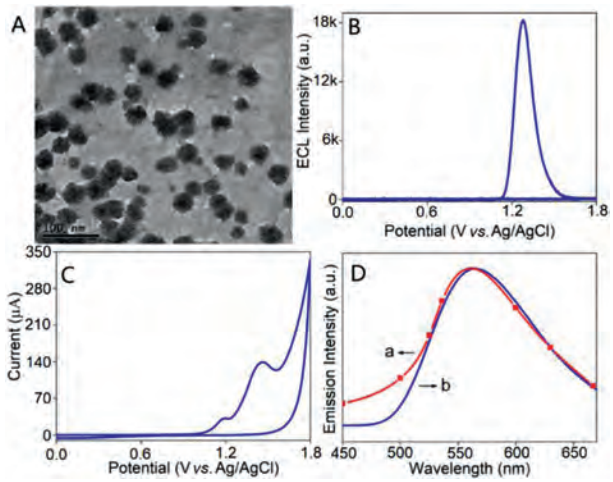

Fig. 1. TEM image (plotting scale: 100 nm) (A), ECL (B), CV (C), ECL spectrum (D, a) and fluorescence spectrum (D, b) of conjugated polymer PNPs modified glassy carbon electrodes (GCEs) in a PBS solution (0.1 mol/L, pH 7.4). PNPs concentration: 100 mg/L, λ_{ex} = 370 nm, scan rate: 100 mV/s, PMT = 800 V.

than that of CV, demonstrating that the obtained ECL signal is reliable. To study the two oxidation peaks in the CV data of conjugated polymer PNPs, the CV of *N*'-hydroxyethanimidamide was measured to give oxidation peaks at +1.18 V and +1.46 V (Fig. S8 in Supporting information), respectively, which is similar to conjugated polymer PNPs. This result suggests that the two oxidation peaks of PNPs can be assigned to the amidoxime group. Furthermore, the CV of ethylenediamine (EDA) gave the oxidization peak around +1.53 V (Fig. S9 in Supporting information), which is similar to the +1.46 V peak of PNPs. This phenomenon can assign the +1.46 V peak to the -NH_2 in amidoxime group while the peak at +1.18 V can be ascribed to the oximido part of amidoxime group.

The model polymer PNPs exhibited non-ECL behavior in a PBS solution (0.1 mol/L, pH 7.4) but strong ECL signal after 25 mmol/L EDA added (Fig. S10 in Supporting information), which can confirm the self-enhanced ECL property of conjugated polymer PNPs. On the other hand, the model polymer PNPs also could not exhibit obvious ECL emission in PBS solution (0.1 mol/L, pH 7.4) with 25 mmol/L acetoxime with only oximido group (Fig. S10 in Supporting information), indicating that the -NH_2 is the effective coreactive part in amidoxime group. It can be observed that the ECL onset potential of conjugated polymer PNPs is 0.23 V lower than that of model polymer PNPs in 25 mmol/L EDA (Fig. 1B and Fig. S8), which can be attributed to the low-oxidation-potential ECL mechanism [18,28]. The ECL mechanism of conjugated polymer PNPs can be summarized as below:

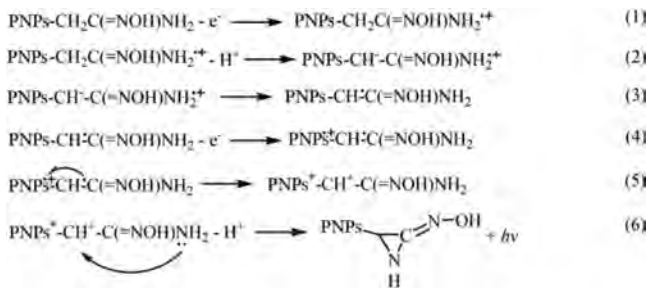

In Fig. 1D, conjugated polymer PNPs gave the ECL emission peak around 563 nm, which is similar to its fluorescence emission spectrum. This result indicated that the ECL process of conjugated polymer PNPs can be assigned to band gap emission mechanism [29].

As is shown in Fig. 2A, the conjugated polymer PNPs gave obviously enhanced ECL signal as UO_2^{2+} concentration increased from 0.1 μg/L to 100 μg/L. As it was reported in previous study, the XPS data proved that the UO_2^{2+} capturing part of amidoxime group is C = N–OH, which could also be confirmed by similar XPS data in Fig. S11 (Supporting information) [25]. In detail, the two peaks centered at 377.2 eV and 391.8 eV in U 4f spectra can confirm the combination of UO_2^{2+} to PNPs (Fig. S11A). While the peaks of C=N-U and N–O-U in Figs. S11B and C proved that the UO_2^{2+} capturing part of this PNPs is C=N–OH. This conclusion can also be demonstrated by the CV data carried out in Fig. 2B. It is obvious that the oxidation peak at +1.18 V (assigned to oximido part of amidoxime group) disappeared when 300 μg/L UO_2^{2+} was added. While on the other hand, the oxidation peak at +1.46 V (-NH_2 group) exhibited no obvious change, demonstrating that UO_2^{2+}

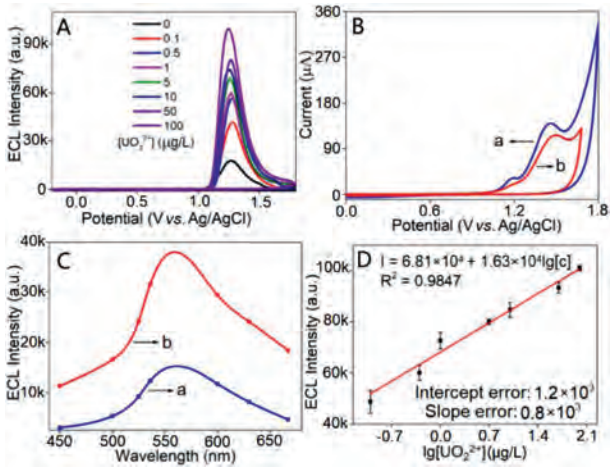

Fig. 2. ECL of conjugated polymer PNPs modified GCEs with different UO_2^{2+} concentration in a PBS solution (0.1 mol/L, pH 7.4) (A); CVs (B) of PNPs; ECL spectra of PNPs (a) and PNPs with 5 μg/L UO_2^{2+} (b) (C); calibration curve of ECL intensity versus logarithm value of UO_2^{2+} concentration (D) in a PBS solution (0.1 mol/L, pH 7.4). PNPs concentration: 100 mg/L, scan rate: 100 mV/s, PMT = 800 V.

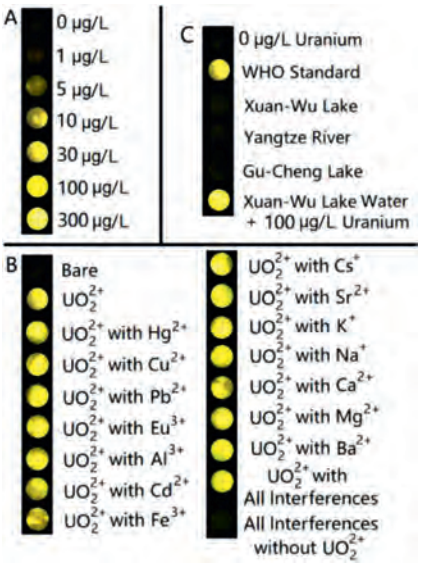

Fig. 3. ECL imaging of conjugated polymer PNPs (A) with different UO_2^{2+} concentration; (B) with 30 μg/L UO_2^{2+} in different interferences (3 mg/L each one); (C) with natural water samples. Polymer concentration 100 mg/L, scan rate: 300 mV/s.

cannot combine with -NH_2 part. This result suggests that the co-reactive amidoxime group of conjugated polymer PNPs cannot be poisoned by UO_2^{2+} in detection process.

The anodic ECL spectrum of UO_2^{2+} has been carried out in 100 mmol/L *N*'-hydroxyethanimidamide as co-reactant to give the emission wave from 460 nm to 580 nm with the emission peak around 500 nm (Fig. S12 in Supporting information). According to the UV–vis absorption spectrum (Fig. S13 in Supporting information), the absorbance wave of conjugated polymer can overlap with the ECL spectrum of UO_2^{2+} in the region from 460 nm to 540 nm. This result demonstrates the existence of the RET process from UO_2^{2+} to conjugated polymer PNPs in ECL detection. Therefore, the UO_2^{2+} captured by amidoxime group can enhance the ECL signal of conjugated polymer PNPs *via* this RET process. To further confirm the RET process, the ECL spectrum of conjugated polymer PNPs was measured after treated with 5 μg/L UO_2^{2+} (Fig. 2C). Similar to conjugated polymer PNPs, the ECL emission peak of conjugated polymer PNPs with 5 μg/L UO_2^{2+} appeared around 563 nm which is different from the ECL spectrum of UO_2^{2+} (Fig. S12). This result confirmed that the ECL emission of conjugated polymer PNPs with 5 μg/L UO_2^{2+} can be assigned to conjugated polymer PNPs instead of UO_2^{2+}, which also confirms the existence of the RET process from UO_2^{2+} to PNPs. The ECL intensity of conjugated polymer PNPs increased obviously after 5 μg/L UO_2^{2+} added. This phenomenon can also be regarded as an evidence of this RET process. On the other hand, conjugated polymers can exhibit excellent conductive property [30]. The combination of UO_2^{2+} with conjugated polymer can probably make PNPs denser than bare ones, which may close the distance between two conjugated chains in PNPs to enhance the conductivity of PNPs. This may be another potential reason of the sharp enhancement of ECL signal after adding UO_2^{2+}. Furthermore, the intensity of ECL signals versus the logarithm value of UO_2^{2+} concentration was carried out in Fig. 2D and gave excellent linearity with an ultra-low LOD of 0.6 ng/L to UO_2^{2+} (0.5 ng/L to U), indicating the ultra-high sensitivity of this probe to UO_2^{2+}. According to previous studies, this LOD value is at least three orders of magnitude lower than the known UO_2^{2+} fluorescent probes while five times lower than the ssDNA based UO_2^{2+} ECL sensor in our previous study (Table S1) [15].

The simplification of pretreatment and data analysis is significant in determining the efficiency of UO_2^{2+} warning especially when rapidly monitoring the UO_2^{2+} in drinking water source. ECL imaging technology can help researchers to compare the UO_2^{2+} concentration with WHO standard by naked eyes, which is beneficial for UO_2^{2+} rapid warning. ITO electrodes were applied in ECL imaging to avoid the complex pretreatment of traditional glassy carbon electrodes (GCEs). As was shown in Fig. 3A, the brightness of conjugated polymer PNPs exhibited gradual enhancement as the concentration of UO_2^{2+} increased from 0 to 300 μg/L, exhibiting the similar trend with the ECL detection data in Figs. 2A and D.

The selectivity of conjugated polymer PNPs was then measured in 3 mg/L different interference ions (Fig. 3B). Among them, Na^+, K^+, Ca^{2+}, Mg^{2+}, Fe^{3+} and Al^{3+} are some common cations in environment. Hg^{2+}, Cu^{2+}, Pb^{2+}, Ba^{2+} and Cd^{2+} were chosen to represent heavy metals. Eu^{3+} can exhibit obvious ECL signal [31] and show relationships with the detection and adsorption of UO_2^{2+} [32]. Cs^+ and Sr^{2+} are two kinds of radioactive elements (^{137}Cs and ^{90}Sr), which often coexist with UO_2^{2+} [33,34]. It can be observed that these interference cations could not obviously affect the response of conjugated polymer PNPs to UO_2^{2+}, indicating the excellent selectivity of this probe. The non-response of these interference ions can be attributed to two reasons: i) their anodic non-ECL property; ii) the excellent UO_2^{2+} selectivity of amidoxime group. Although Eu^{3+} could exhibit obvious ECL signal in cathodic region, it could not affect the detection of UO_2^{2+} due to its non-ECL behavior in anodic region [31,35]. On the other hand, the salinity of the natural water sample is also a potential factor to affect the detection results. Therefore, ECL images of conjugated polymer PNPs with 30 μg/L UO_2^{2+} in water samples with different salinity were taken and listed in Fig. S14 (Supporting information). It is obvious that neither natural fresh water nor the prepared water samples with high salinity could affect the detection of UO_2^{2+} (the salinity of fresh water was known as 10–500 mg/L). Besides, 0.1 and 10 μg/L UO_2^{2+} solution with 3 mg/L each interfering ion have been measured (Fig. S15 in Supporting information) to give the results as 0.10 and 9.77 μg/L, respectively. The relative standard deviation (RSD) values were given as 2.3% and 0.6%, respectively. These results demonstrate the reliability of UO_2^{2+} determination in complex samples. As a natural water sample, the concentration of uranium was known as around 3.3 μg/L in seawater [36,37], which was measured as 3.80 μg/L by this sensor with the RSD of 1.9% (Fig. S15). This result further confirmed the application of this sensor in practical natural water samples.

Furthermore, the UO_2^{2+} rapid warning system was applied in some natural water samples to confirm its practicality. Some fresh water samples have been collected from Xuan-Wu Lake (Nanjing, China), Gu-Cheng Lake (Nanjing, China) and Yangtze River (Yangzhou, China), respectively. According to the WHO standard of drinking water, the concentration of UO_2^{2+} cannot exceed 30 μg/L, which was chosen as the standard group in UO_2^{2+} rapid recognition. In Fig. 3C, the UO_2^{2+} concentration values of these three water sources are all in safe region comparing with the WHO standard. But when 100 μg/L UO_2^{2+} was added in Xuan-Wu Lake water, the brightness of conjugated polymer PNPs exhibited a sharp enhancement, which is brighter than WHO standard. The result demonstrates that this UO_2^{2+} warning system can rapidly and simply recognize the exceeding UO_2^{2+} in drinking water sources by naked eyes, which is meaningful in the water safety early warning for public security.

In summary, a conjugated polymer with self-enhanced ECL behavior was synthesized and prepared into PNPs for UO_2^{2+} rapid warning in drinking water source. This study discovered that amidoxime group, a most successful UO_2^{2+} capturing group, can also be applied as a co-reactive group in ECL measurement, indicating its bi-functional property. The captured UO_2^{2+} could enhance the ECL signal of conjugated polymer PNPs *via* RET process, which gave an ultra-low LOD value as 0.5 ng/L to U as well as high selectivity. ECL imaging technique was then successfully applied in this UO_2^{2+} warning system to realize visualized natural water source rapid monitoring. This study reported a novel strategy for UO_2^{2+} rapid warning in drinking water sources and exhibited its practical applications in environmental and public security fields.

Declaration of competing interest

The authors declare that they have no known competing financial interests or personal relationships that could have appeared to influence the work reported in this paper.

Acknowledgments

This work was financially supported by the National Natural Science Foundation of China (Nos. U1867206, 21906115), State Key Laboratory of Analytical Chemistry for Life Science (No. SKLACLS2014), the China Postdoctoral Science Foundation (No. 2020T130456) and the Priority Academic Program Development of Jiangsu Higher Education Institutions (PAPD).

Supplementary materials

Supplementary material associated with this article can be found, in the online version, at doi:10.1016/j.cclet.2021.11.019.

References

[1] C. Liu, P.C. Hsu, J. Xie, Nat. Energy 2 (2017) 8.
[2] L. Farzin, M. Shamsipur, S. Sheibani, L. Samandari, Z. Hatami, Microchim. Acta 186 (2019) 289.
[3] Y.C. Yue, M.H. Li, H.B. Wang, B.L. Zhang, W. He, Environ. Health Prev. 23 (2018) 18.
[4] X. Qin, W. Yang, Y. Yang, Inorg. Chem. 59 (2020) 9857–9865.
[5] M.A. Abu-Dalo, N.A.F. Al-Rawashdeh, I.R. Al-Mheidat, N.S. Nassory, Sens. Actuat. B: Chem. 227 (2016) 336–345.
[6] Z. Jiang, H. Li, R. Ai, Y. Deng, Y. He, ACS Sustain. Chem. Eng. 8 (2020) 11630–11637.
[7] P. Wu, K. Hwang, T. Lan, Y. Lu, J. Am. Chem. Soc. 135 (2013) 5254–5257.
[8] W. Miao, Chem. Rev. 108 (2008) 2506–2553.
[9] J.M. Wong, R. Zhang, P. Xie, Angew. Chem. Int. Ed. 59 (2020) 17461–17466.
[10] H. Gao, N. Zhang, J.B. Pan, ACS Appl. Mater. Interfaces 12 (2020) 54012–54019.
[11] Y. Nie, X. Tao, H. Zhang, Y.Q. Chai, R. Yuan, Anal. Chem. 93 (2021) 3445–3451.
[12] F. Sun, Z. Wang, Y. Feng, et al., Biosens. Bioelectron. 100 (2018) 28–34.
[13] J. Zhao, Y.M. Lei, Y.Q. Chai, R. Yuan, Y. Zhuo, Biosens. Bioelectron. 86 (2016) 720–727.
[14] Y.M. Lei, M. Zhao, A. Wang, et al., Chem. Eur. J. 22 (2016) 8207–8214.
[15] Z. Wang, J.B. Pan, Q. Li, et al., Adv. Funct. Mater. 30 (2020) 2000220.
[16] N. Wang, Z. Wang, L. Chen, et al., Chem. Sci. 10 (2019) 6815–6820.
[17] S. Voci, B. Goudeau, G. Valenti, et al., J. Am. Chem. Soc. 140 (2018) 14753–14760.
[18] N. Wang, H. Gao, Y. Li, Angew. Chem. Int. Ed. 60 (2021) 197–201.
[19] Y. Liu, W. Guo, B. Su, Chin. Chem. Lett. 30 (2019) 1593–1599.
[20] H. Wang, Y. Yuan, Y. Zhuo, Y. Chai, R. Yuan, Anal. Chem. 88 (2016) 2258–2265.
[21] Q. Ding, M. Zhu, H. Deng, R. Yuan, Y. Yuan, Biosens. Bioelectron. 184 (2021) 113227.
[22] S. Zhao, Y. Yuan, Q. Yu, et al., Angew. Chem. Int. Ed. 58 (2019) 14979–14985.
[23] B. Yan, C. Ma, J. Gao, Y. Yuan, N. Wang, Adv. Mater. 32 (2020) 1906615.
[24] M. Xu, T. Wang, P. Gao, et al., J. Mater. Chem. A 7 (2019) 11214–11222.
[25] M. Xu, X. Han, D. Hua, J. Mater. Chem. A 5 (2017) 12278–12284.
[26] N. Wang, Y. Feng, Y. Wang, H. Ju, F. Yan, Anal. Chem. 90 (2018) 7708–7714.
[27] Z. Wang, S. Liu, Y. Wang, Y. Quan, Y. Cheng, Macromol. Rapid Commun. 38 (2017) 1700150.
[28] G. Valenti, S. Scarabino, B. Goudeau, 139, J. Am. Chem. Soc. (2017) 16830–16837.
[29] H. Gao, N. Zhang, Y. Li, Sci. China Chem. 63 (2020) 715–721.
[30] G.E.J. Hicks, S. Li, N.K. Obhi, C.N. Jarrett-Wilkins, D.S. Seferos, Adv. Mater (2021) 2006287.
[31] L. Deng, Y. Shan, J.J. Xu, H.Y. Chen, Nanoscale 4 (2012) 831–836.
[32] M.F. Hamza, J.C. Roux, E. Guibal, Chem. Eng. J. 344 (2018) 124–137.
[33] T.L. Babich, A.V. Safonov, D.S. Grouzdev, Microbiology 88 (2019) 613–623.
[34] A. Espriu-Gascon, J. Gimenez, I. Casas, J. de Pablo, J. Hazard. Mater. 353 (2018) 431–435.
[35] Q. Jiang, M. Hakansson, A.M. Spehar, et al., Anal. Chim. Acta 558 (2006) 302–309.
[36] Y. Oyola, C.J. Janke, S. Dai, Ind. Eng. Chem. Res. 55 (2016) 4149–4160.
[37] Y. Yue, R.T. Mayes, G. Gill, RSC Adv. 5 (2015) 50005–50010.